MASSACHUSETTS INSTITUTE OF TECHNOLOGY

APOLLO

GUIDANCE, NAVIGATION AND CONTROL

E-1942

COMMAND ANGLE TORQUING OF GYROS IN THE APOLLO GUIDANCE AND NAVIGATION SYSTEM

by
Maurice Lanman and Julius Feldman

April 1966

MIT INSTRUMENTATION LABORATORY
CAMBRIDGE 39, MASSACHUSETTS

MASSACHUSETTS INSTITUTE OF TECHNOLOGY

APOLLO

GUIDANCE AND NAVIGATION

Approved: John E Miller Date: 20 May 66
JOHN E. MILLER, DIRECTOR, ISS
APOLLO GUIDANCE AND NAVIGATION PROGRAM

Approved: David G Hoag Date: 20 May 66
DAVID G. HOAG, DIRECTOR
APOLLO GUIDANCE AND NAVIGATION PROGRAM

Approved: Ralph R Ragan Date: 23 May 66
RALPH R. RAGAN, DEPUTY DIRECTOR
INSTRUMENTATION LABORATORY

To be presented at:

Instrument Society of America
Aerospace Instrumentation Symposium,
Marriott Motor Hotel,
Philadelphia, Pa.
May 2, 1966

E-1942

COMMAND ANGLE TORQUING OF GYROS IN THE APOLLO GUIDANCE AND NAVIGATION SYSTEM

by
Maurice Lanman and Julius Feldman

April 1966

MIT INSTRUMENTATION LABORATORY
CAMBRIDGE 39, MASSACHUSETTS

COPY # 16

ACKNOWLEDGEMENT

This report was prepared under DSR Project 55-238, sponsored by the Manned Spacecraft Center of the National Aeronautics and Space Administration through Contract NAS 9-4065.

Credit is given to James Sitomer who developed the pulse command circuitry, to the Electromagnetic Group who developed the magnetic suspension and torque generator, to John E. Miller who implemented the technique as used by the Apollo Guidance and Navigation System and to many other groups and individuals at MIT/IL for their contribution to the technique discussed in this paper.

E-1942

COMMAND ANGLE TORQUING OF GYROS IN THE APOLLO GUIDANCE AND NAVIGATION SYSTEM

ABSTRACT

The Apollo Guidance and Navigation System stable platform is positioned by digitally torquing the floats of the gyroscopes. Command angle torquing to an accuracy of 0.1 percent can be obtained with this technique. System implementation is discussed in general; the mechanics of torquing the gyro float and the precision torquing techniques are detailed. Results of investigation into various phenomena which affect accuracy and repeatability are reported.

by Maurice Lanman
Julius Feldman

April 1966

TABLE OF CONTENTS

INTRODUCTION

To accurately position the Apollo Guidance System gimbals during prelaunch and in flight the gyros are electrically torqued. Gyro torquing is also performed to compensate for the in flight gyro drift terms. Torquing is commanded by the guidance computer as a pulse train of equal pulse width spacing. This method quantizes gimbal command angles; a single pulse to a gyro commands a 0.6 second of arc gimbal displacement.

We will discuss the methods used to perform this command torquing in the Apollo Guidance and Navigation System, the Apollo Gyroscope, the gyro torque generator, and some of the sources of error that this method of torquing can obtain.

THE GYROSCOPE

The gyro used in this system is a single degree of freedom integrating gyro (See Figure 1). A synchronous hysteresis motor running at 24,000 rpm supplies the gyro angular momentum.

The motor is hermetically sealed into a spherical chamber. This chamber is surrounded by high density Brominated Fluorocarbon. The gyro unit is temperature controlled to 135^{o}F to maintain the spherical float in approximately neutral buoyancy.

At each end of the float is an electromagnetic suspension. The suspension minimizes the relative motion, both axial and radial, between the float and the case when the gyro case is accelerated.

On one end of the gyro float is a signal generator. Its output is a 3200 cps voltage whose magnitude is proportional to the angular displacement of the float about the output axis.

On the other end of the float is a torque generator. With a current input, a torque is developed on the float about the gyro output axis.

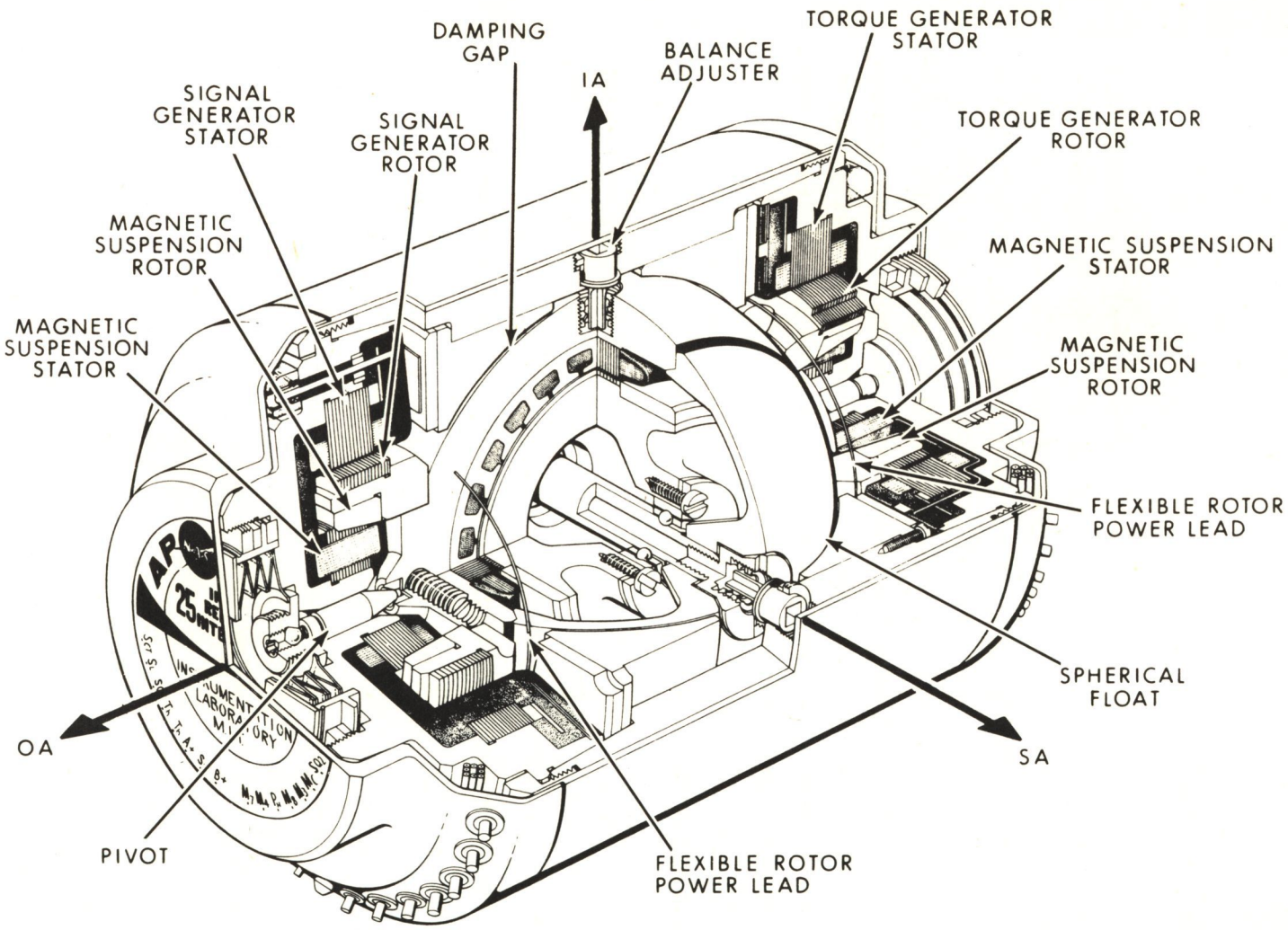

Fig. 1 Apollo II IRIG

SYSTEM DESCRIPTION

The input axes of three gyros are aligned along the three gimbal axes of the Apollo Inertial Measurement Unit. The signal generator signals control the gimbal drive motors. This loop rotates the gyro cases about their input axes to maintain the gyro floats at null due to spacecraft angular rates or torques on the gyro float. Gyro torques may be caused by a non coincidence of the center of gravity and center of buoyancy of the float causing an acceleration sensitive torque, gravity insensitive (bias) torque, or torques created by current inputs to the torque generator. Without these torque inputs the gimbal system will remain fixed in inertial space regardless of spacecraft motion.

With the gyro output axis maintained at null by the gimbal stabilizing loop (Figure 2) the gyro equation can be written as:

$$M_{OA} = \dot{A}_{IA} \times H \tag{1}$$

Where

M_{OA} = the torque on the gyro float about the output axis (dyne-cm)

$\dot{A}_{IA}$ = the angular velocity of the gyro case about its input axis with respect to inertial space (radians/sec)

H = the gyro angular momentum ($gm\text{-}cm^2/sec$)

Integrating both sides of equation (1) obtains:

$$A_{IA} = \frac{1}{H} \int M_{OA}\, dt \tag{2}$$

This equation shows the basic operation of the gyro loop. The angular drift of the gimbal about the gyro input axis will be proportional to the integral of the torque on the gyro float.

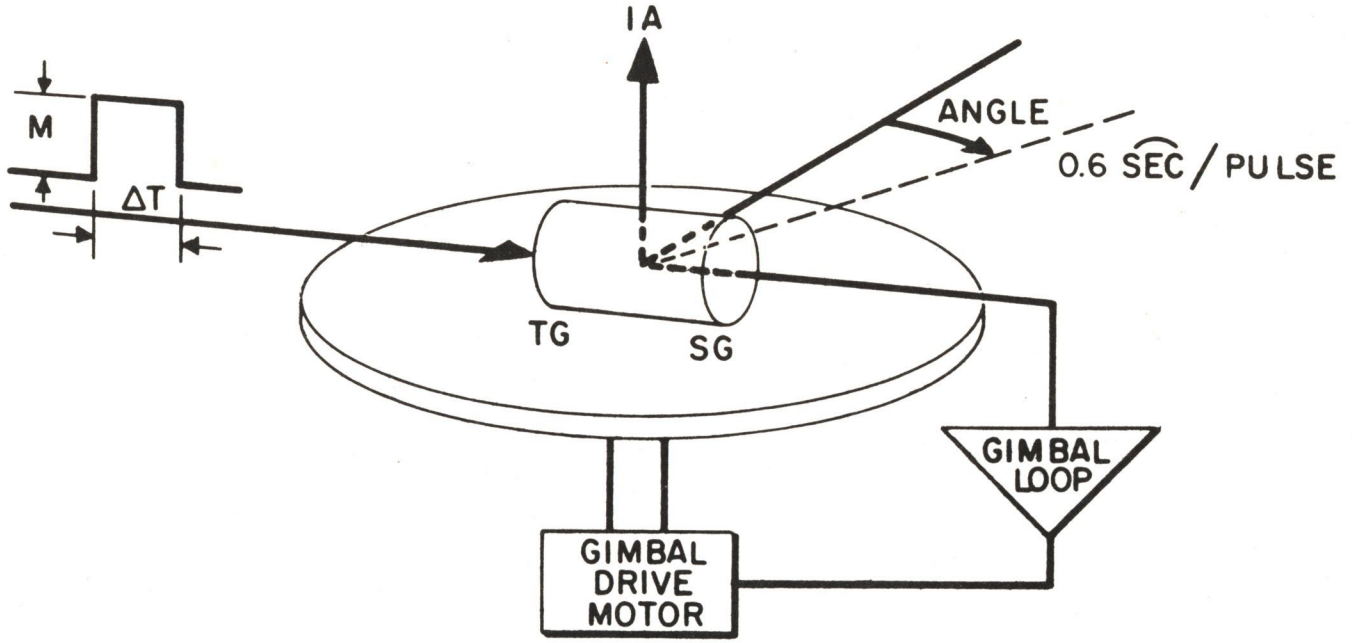

PULSE TORQUE SCALE FACTOR $\left(\frac{mr}{PULSE}\right)$

= THE ANGLE THE GYRO INPUT AXIS IS COMMANDED THROUGH DUE TO A PULSE TO THE TORQUER

$$SF = \frac{M\Delta T}{H} \quad \left(\frac{mr}{PULSE}\right)$$

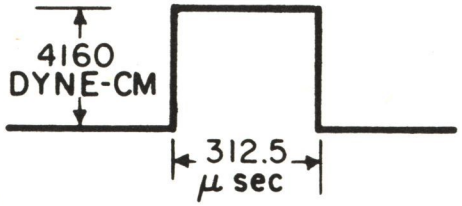

Fig. 2 Gyro Pulse Torquing Scale Factor

TP14295

In the Apollo Guidance and Navigation System, the Guidance Computer determines the quantity of angular command required for the three gimbal axes. DC current, accurately controlled in magnitude and duration, is applied to the torque generator, to produce a precisely known torque-time integral, and through the gyro and loop dynamics (See Equation 2), a precisely known quantity of gimbal angular rotation.

THE TORQUE GENERATOR

An elementary, eight pole, bidirectional torque generator is shown schematically in Figure 3. Alternate poles are designated as plus and minus. (Energizing the "plus" or "minus" poles produces positive or negative torque, respectively.) The rotor is a four pole device, each pole covering half of two stator poles. There is one winding on each of the eight stator poles; all windings on the plus poles (1, 3, 5, 7) or on the minus poles (2, 4, 6, 8) are excited simultaneously. Note that windings on alternate plus or minus are wound opposite (i.e. 1 and 5 are north, 3 and 7 south poles).

The stator core and rotor are constructed from stacked laminations of ferromagnetic material. Actual dimensions of the Apollo torquer are also given in Figure 3.

Note also, that the torque generator is the outer half of a ducosyn, the inner half being the gyro float magnetic suspension (radial and axial). (These circuits are magnetically isolated by a beryllium ring dividing the rotor).

THEORY OF OPERATION

When DC current is supplied to one set of windings (either "plus" or "minus") flux is generated in the corresponding set of air gaps. The arrangement of the rotor poles and slots results in a gap energy gradient with rotor position, and torque is produced on the rotor.

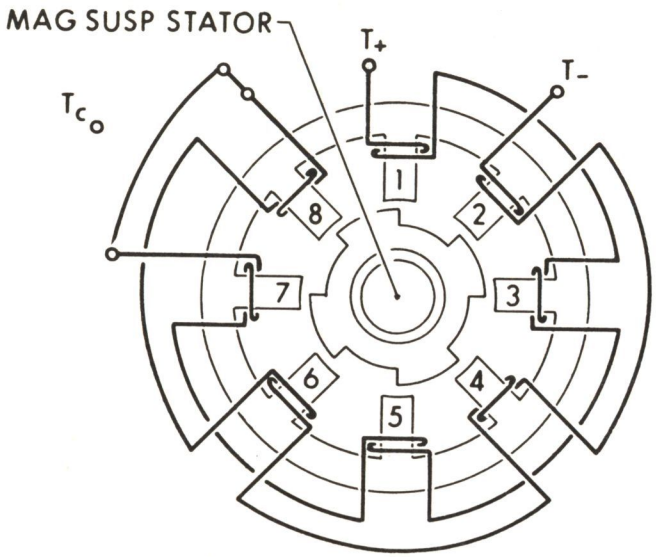

TORQUER SCHEMATIC INCLUDING WINDINGS

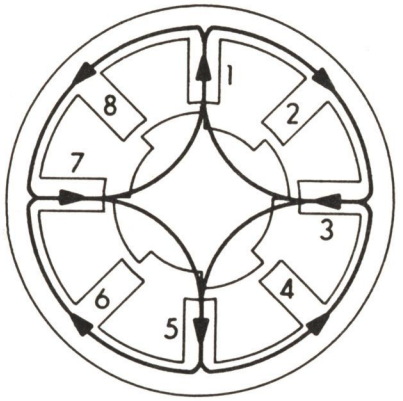

TORQUER SCHEMATIC SHOWING FLUX PATHS FOR PLUS TORQUING

OVERALL DIAMETER	1.750 inch
WIDTH OF STATOR POLES	0.137 inch
DEPTH OF STATOR POLES	0.228 inch
DIAMETER OF ROTOR	0.982 inch
GAP LENGTH	0.010 inch
DEPTH OF ROTOR SLOTS	0.062 inch
NO. OF WINDINGS PER POLE	350 turns

TABLE OF DIMENSIONS

Fig. 3 Apollo I Torque Generator Schematics and Dimensions

The general equations for magnetic torque are developed as follows:

$$W_{fld} = 1/2\ F\phi(\theta) = 1/2\phi^2(\theta)R(\theta) \tag{3}$$

$$M_{OA} \sim dW_{fld}/d\theta = -\ 1/2\phi^2(\theta)dR(\theta)/d\theta \tag{4}$$

Where:

W_{fld} = field energy
F = mmf
ϕ = flux
θ = angular displacement of rotor
R = reluctance

The torque, M_{OA}, is proportional to the square of the flux, ϕ. Since flux-mmf characteristics of air gaps are essentially linear, the flux is directly proportional to the winding current, I, and the number of terms, N:

$$\phi(\theta) = F/R(\theta) = NI/R(\theta) \tag{5}$$

and

$$M_{OA\,(TG)} \sim \left[N^2I^2/R^2(\theta)\right]\ dR/d\theta \tag{6}$$

The torque is translated into float motion about the gyro output axis, an error signal is generated by the signal generator, which through a high gain servo loop, drives the stable platform about the gyro input axis. Motion about the gyro input axis produces an opposite torque about the gyro output axis, driving the float back to null.

From equation (1) we find the torque produced through the gyro dynamics is:

$$M_{OA\,(GD)} \sim H\dot{A}_{IA}$$

Balancing the torque requires that:

$$M_{OA\,(GD)} = M_{OA\,(TG)} \tag{8}$$

therefore,

$$\dot{A}_{IA} \sim \frac{N^2}{H} \cdot \frac{1}{R^2} \cdot \frac{dR}{d\theta} \cdot I^2 \tag{9}$$

and

$$A_{IA} \sim \frac{N^2}{H} \cdot \frac{1}{R^2} \cdot \frac{dR}{d\theta} \int I^2\,dt \tag{10}$$

The angular velocity, $\dot{A}_{IA}$, and net angular motion, A_{IA}, of the platform are related to the torquer parameters by equations (9) and (10).

Since the purpose of torquing the gyro is to accurately position the platform, it is necessary to precisely control the terms on the right-hand side of the equation (10). The terms N and H are built into the gyro and are invariant. The control of (I^2dt), which is the heart of digital torquing technique, will be discussed in a following section.

Except for a few special effects, which will also be dealt with later, the remainder of the problem can be lumped into controlling the reluctance dependent term, $(dR/d\theta)/R^2$

RELUCTANCE DEPENDENT TORQUE VARIATIONS

Absolute control of the reluctance, beyond the limits of the mechanical tolerances involved is not attempted, since minor differences in sensitivity from torquer to torquer and from plus to minus torquing can be removed by adjusting the current input for each particular set of windings.

It is necessary, however, to assure that variation of the reluctance dependent term is minimal.

The gap reluctance is related to the torquer geometry as follows:

$$R(\theta) = \frac{\mu g\ (g + d)/b}{(2g + d)\, a/2 + (r\theta)d} \tag{11}$$

Where

μ = permeability of gap fluid
g = gap length
d = slot depth
b = stator pole depth
a = stator pole width
r = radius of air gap

This equation is of the form:

$$R(\theta) = A/(B + C\theta) \tag{12}$$

therefore

$$dR(\theta)/d\theta = -AC/(B + C\theta)^2 \tag{13}$$

and

$$\frac{dR(\theta)}{d\theta} \cdot \frac{1}{R^2\ (\theta)} = -\frac{C}{A} \tag{14}$$

$$M_{OA} \sim C/A \sim \frac{drb}{g\,(g + d)} \tag{15}$$

The torque, M_{OA}, then is a function only of gap length, g, slot depth, d, pole depth, b, gap radius, r, and permeability.

Theoretically, the torque is independent of rotor displacement, θ, and no elastic restraint will be observed. In actuality, however, there is an elastic restraint on the order of 300 ppm (.03%) per milliradian of rotor motion. It is suspected that changes in fringing fields, irregularities in pole and rotor surfaces (such as ellipticity of the rotor), and variations in gap length with rotation (see following paragraphs) are major contributors. Since the servo loop holds the rotor null to much better than a milliradian under normal conditions, this effect becomes negligible.

The only first order geometrical variable in the torque equation, then, is the gap length, g; the terms b, d, and r are mechanical characteristics of the rotor and stator.

When the torque generator is energized, it produces a radial force on the rotor which acts as a negative spring constant (the displacing force increased with radial displacement). This force is proportional to the square of the torquer current, I, and to the displacement of the rotor from center. It opposes the radial restoring force generated by the magnetic suspension. If the suspension stator and torquer stator are not exactly concentric, there will be radial motion of the rotor and a subsequent change in gap lengths when current is applied to the torquer. The amount of change is dependent upon the average current supplied to the torquer and the magnitude of the misalignment of the centers. This effect, illustrated in Figure 4, is called radial side-loading.

This simplified analysis shows that side-loading produces a second order nonlinearity in the torque equation by making the gap length a function of current. It can be controlled by maintaining a tight concentricity between torquer and suspension, and a very high suspension stiffness and since precision torquing is required only for small average currents, by calibrating the torquers at low level average current, where there is little side-loading.

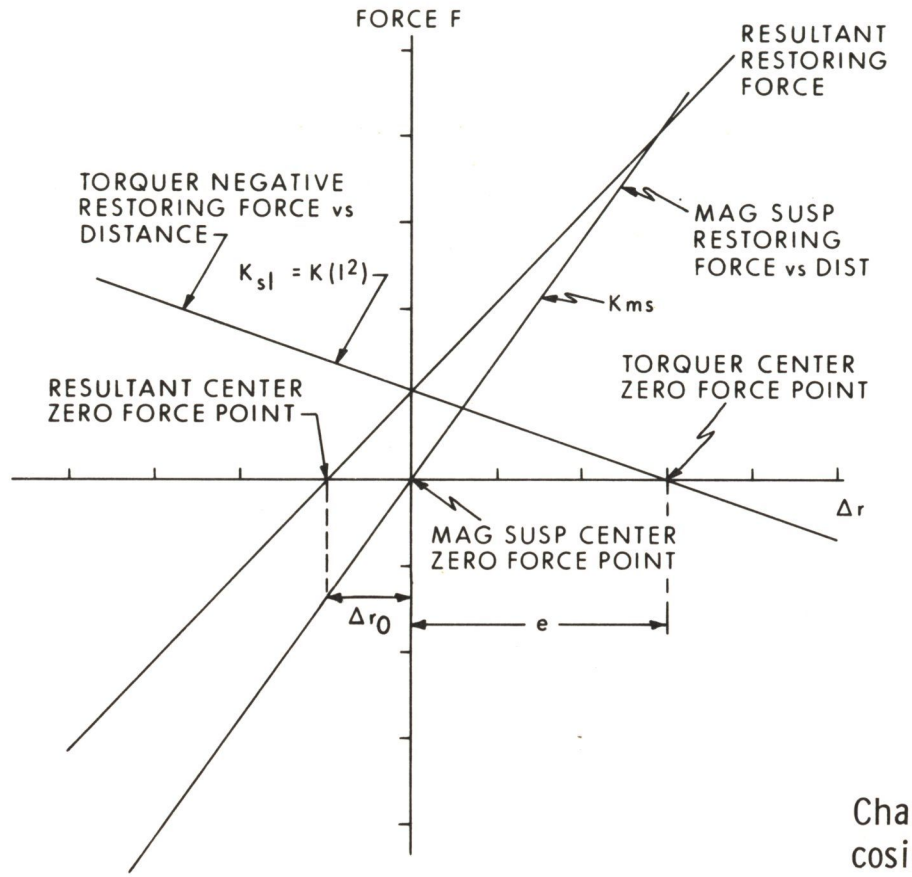

$$F_{ms} = K_{ms}\Delta r$$

$$F_{sl} = -K_{sl}(\Delta r - e)$$

$$F_{ms} + F_{sl} = 0 = (K_{ms} - K_{sl})\Delta r + K_{sl}e$$

$$\Delta r_{F=0} = \frac{-K_{sl}e}{K_{ms} - K_{sl}}$$

K_{ms} must be greater than K_{sl} for stable center

$$\Delta r_0 = \frac{-KI^2e}{K_{ms} - KI^2}$$

$$\Delta g_n \sim \Delta r_0 \cos\left(\frac{2n\pi}{8} + \theta\right)$$

Change in gap of pole n is proportional to the cosine of its angular displacement from the direction of Δr_0.

Fig. 4 Side Loading Due to Torquer Negative Restraint

For the Apollo torquer, a 100μ-inch radial centering error (1% of the gap length) has been found to produce torque errors of less than 1000 ppm (0.1%) even with full current applied.

Note also that radial centering errors may contribute to the observed elastic restraint. If the rotor and stator are not concentric, the average gap length, g, will not be constant under a given pole, but will vary with angular displacement, θ; the torque equation will no longer be independent of θ.

Axial side loading also prevents somewhat of a problem under certain conditions. If the rotor and stator are not axially aligned, there will be a tendency to align when current is applied to the torquer. This aligning force, again, opposes the force provided by the axial suspension. As the realigning takes place, the effective gap is changing, and a subsequent change in torque output is observed. The amount of overall axial displacement is proportional to the torquer average current, providing another source of torque nonlinearity with current.

This effect is reduced to insignificance in the Apollo gyro by making the rotor poles wider (axially) than the stator poles. The only aligning force (or axial sideloading force) then is provided by fringing fields and very little net motion is observed. In any case, the torquer gap remains constant, except for grossly misaligned units.

RESIDUAL TORQUES

Non-linearities in the stator core and rotor iron cause a residual flux when the current is turned off. The paths of this flux, of course, depend on the previous state of the torquer (i.e. whether torquing plus or minus). The residual torque difference between post-plus and post-minus torquing is small, about .01% of the torque applied when excited; this, however, is enough to significantly affect the gyro's bias drift. (Bias drift is the gravity-independent drift term). Since bias drift is the most

critical performance characteristic of the gyro for the Apollo environment, it is very undesirable to have it seriously affected by the torquing history of the gyro.

Several techniques have been used to reduce or eliminate the residual problem. The most practical involves introducing AC flux into the torquer which, while completely decoupled from the DC torquing windings, wipes the entire stator and rotor maintaining a constant residual regardless of torquing history. One method of accomplishing this is pictured schematically in Figure 5. To be effective, the AC flux must cover all the iron, must be several times the magnitude of expected residuals, and the windings must be wound such that no net voltage is induced in the torquing coils. This method, in general, reduces residual torque by a factor of ten.

OTHER EFFECTS

The preceding discussion has assumed that the reluctance of the stator and rotor iron is invariant or negligible when torquing; however, iron flux-mmf characteristics are very non-linear and poor mechanical design or choice of materials can result in a significant degradation of repeatability. With improved design techniques and the superposition of AC flux in all the poles, this problem has been all but eliminated from the Apollo torque generator.

Internal temperature variation also affects the flux-mmf characteristics of the torquer. Torque output has been found to change by 100 to 300 ppm per degree Fahrenheit. It is suspected that the temperature sensitivity is due to magnetostriction effects caused by stresses on the stator core which result from expansion and shrinkage with temperature of the potting compound encasing the torquer stator. Gyro internal temperature, however, is controlled to within $1^{\circ}F$ in the Apollo system, reducing this effect to a minor consideration.

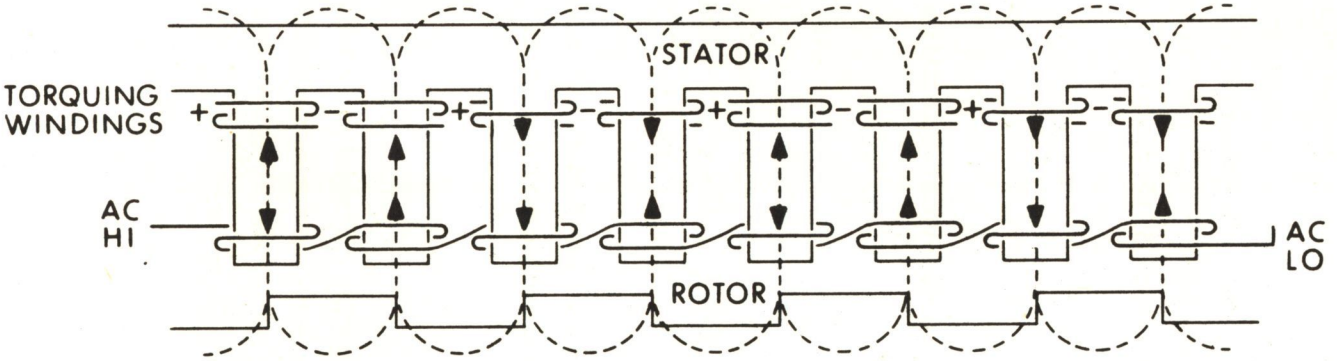

Fig. 5 AC Windings and Wiping Flux

TORQUER CURRENT CONTROL

As shown in the preceding section, the torque about the gyro output axis can be given by

$$M_{OA\,(TG)} = S_{TG}\, I^2 \tag{16}$$

and

$$A_{IA} = \frac{S_{TG}}{H} \int I^2\, dt \tag{17}$$

where S_{TG} is the torque generator sensitivity and is equal to:

$$\frac{N^2}{R^2} \cdot \frac{dR}{d\theta}$$

Therefore, the commanded angle of the gimbal system (A_{IA}) about the gyro input axis is proportional to the area under the square of the current-time curve.

From equation (17) it is apparent that an accurate control of gimbal command angle requires accurate control of both torquer current and torquing time.

CIRCUIT DESCRIPTION

One of the methods used to command torque the three gyros in our gimbal system is to have one set of torquing electronics shared by the three gyros.

This set of torquing electronics consists of Calibration Module, Binary Current Switch, a DC Amplifier, and Precision Voltage Reference. A block diagram of these components is shown in Figure 6.

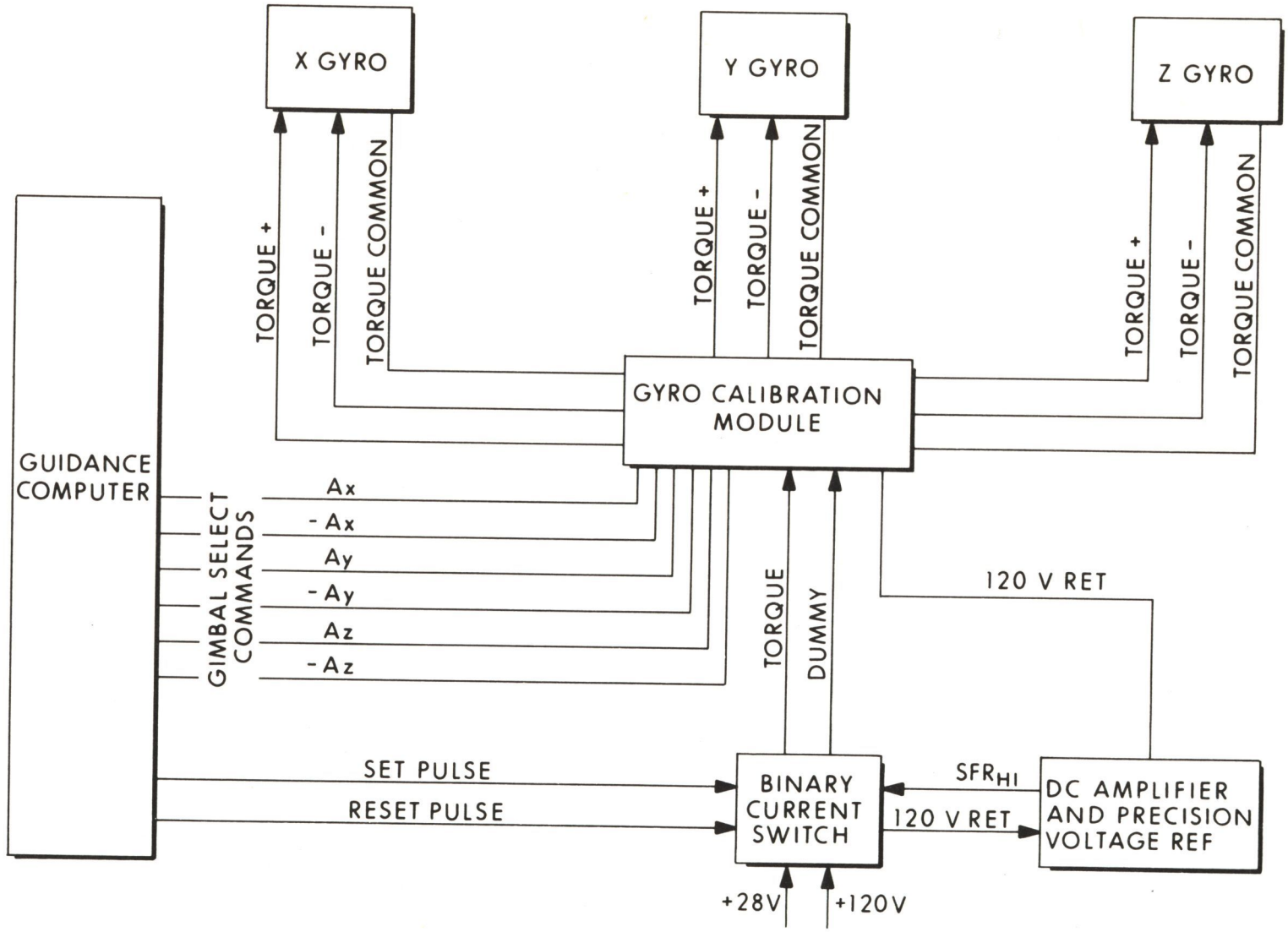

Fig. 6 Block Diagram - Command Angle Torque Loop

The Guidance Computer selects the gimbal axis and direction to be commanded. A string of pulses from the Guidance Computer to the Calibration Module connects the required gyro torque generator to the torquing electronics.

A set pulse from the computer turns on the Binary Current Switch and allows current to flow. A reset pulse to the Switch terminated the current flow.

The spacing between the set and reset pulses are 312.5N microseconds when N is the integer number of command pulses. With N equal to one, the gimbal angle commanded is 0.6 seconds of arc.

When the Guidance Computer turns off its select pulses, the torque generator winding is disconnected from the Calibration Module and the computer is available for other commands.

The DC Amplifier and Precision Voltage Reference are used to obtain an accurate and stable level of torque generator current. When select pulses have been sent by the computer, the Calibration Module is connected to the required torque generator winding as shown in Figure 7. The resistor in series with the torque generator and the parallel resistor capacitor circuit form parallel branches which have equal time constants ($\frac{L}{R} = RC$). In this way the load on the Binary Current Switch is resistive, in order to guarantee DC Amplifier stability. In addition, switching transients are practically eliminated.

The difference between the voltage across the scale factor resistor (SFR) and the six volt Precision Voltage Reference is amplified by the DC Amplifier to control the current flow of the Binary Current Switch.

The Precision Voltage Reference (PVR) is a cascaded zener diode voltage source. Voltage deviation of less than 10 ppm/year is obtained from this PVR. The scale factor resistor is a 100 ppm accuracy resistor

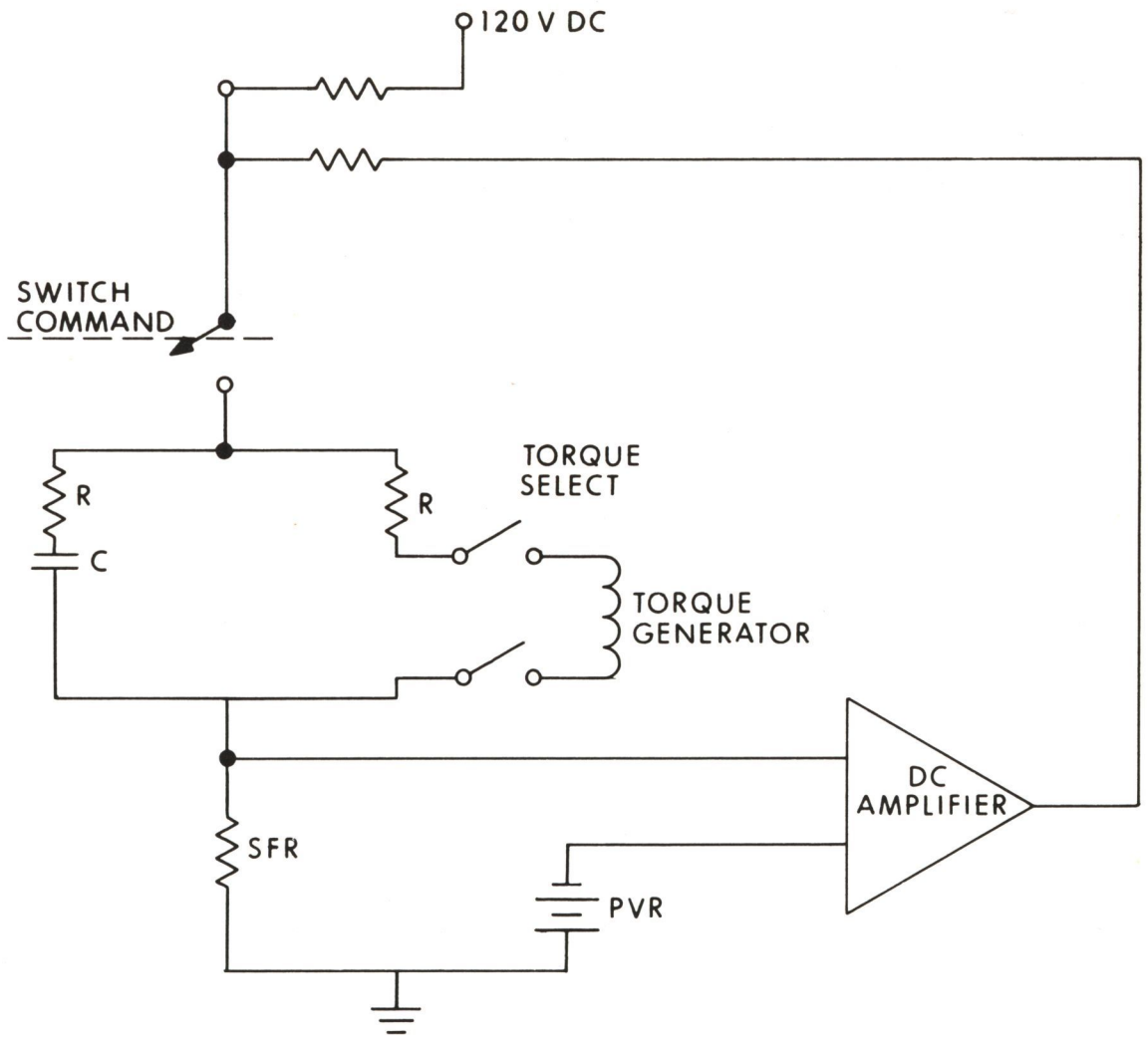

Fig. 7 Torquer Current Control Loop

with a stability of better than 3 ppm/year. These components and the high gain of the DC Amplifier (200,000) insures a torque generator current change of less than 20 ppm/year and a current accuracy of about 100 ppm.

So that gyros in any gimbal axis or system will command the same angle, the torque generator windings are normalized during component acceptance testing. This consists of installing resistors on the gyro end caps to shunt the torquer windings. The resistors are selected to give within 1000 ppm of the same command angle rate for all gyro units.

SCALE FACTOR CHANGE WITH PULSE BURST LENGTH

The inductance of the torque generator causes a command scale factor error that varies with the length of commanded angle.

With a square wave input from the current switch, the current flow through the torque generator winding will be as shown in Figure 8. Equation (17) showed that the commanded gimbal angle is proportional to the area under the square of the current time curve.

The current rise time associated with the torquer inductance results in a smaller area under a single current-squared pulse than the area under the middle pulse of a long string.

The commanded gimbal angle (A_{IA}) for the command time (T) much less than the torque generator time constant (τ) will become:

$$A_{IA} = \frac{S_{TG}}{H} I^2 \cdot (T - \tau) \qquad (18)$$

The scale factor for a single pulse in our system is approximately 80% of the scale factor per pulse of an infinite string of pulses.

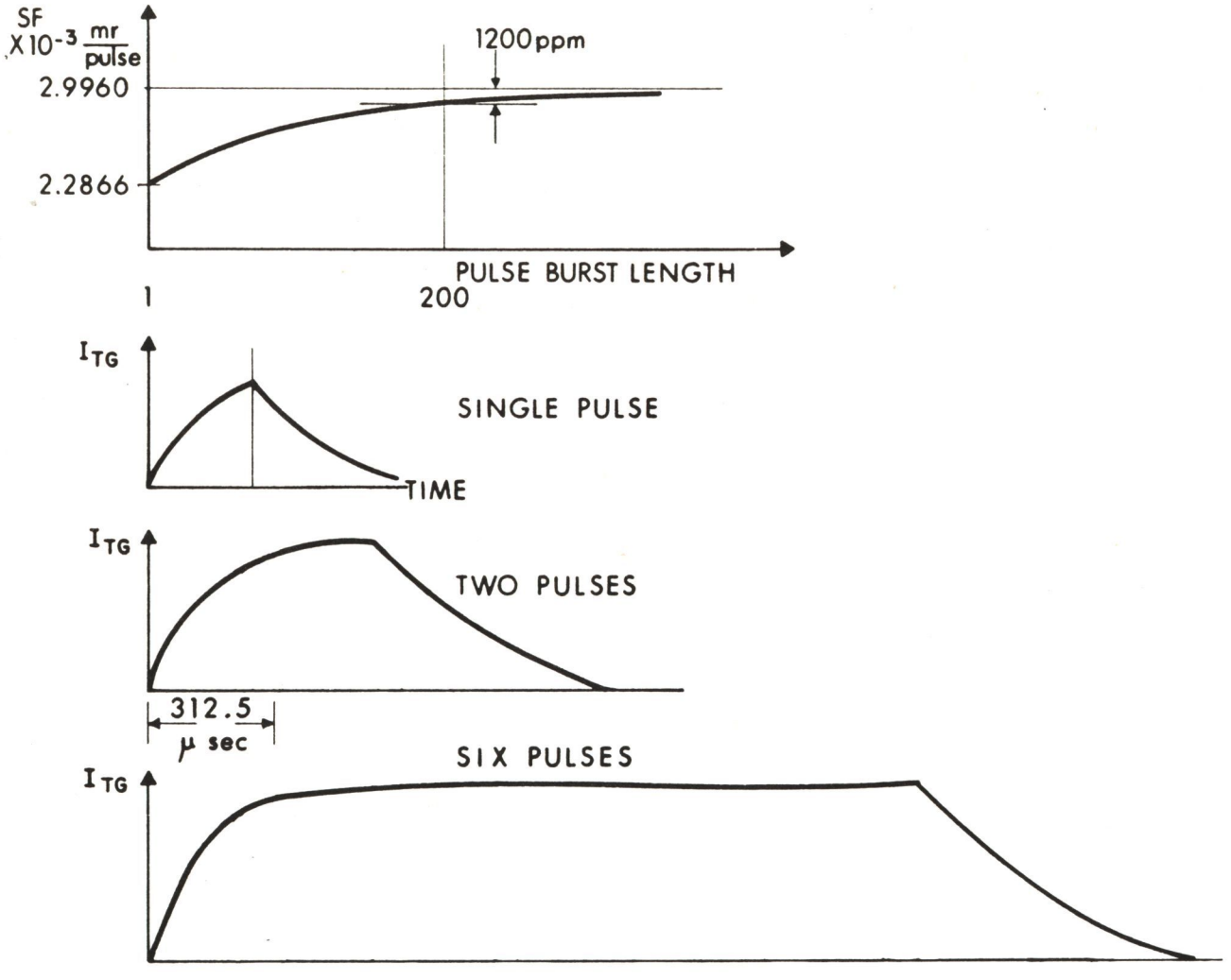

Fig. 8 Pulse Burst Data

The two techniques used to minimize this problem are:

a) torquing the positive and negative torque generator windings at periodic intervals with equal quantities of pulses. The net torque for this condition should be zero. When a command is required, it is inserted in the proper side of of the bidirectional pulses and the effect of the rise time is decreased.

b) The computer accounts for the lower command angle scale factor of a single pulse, and calculates the actual commanded angle due to a string of pulses.

SUMMARY

This concludes the discussion of the major elements and problem areas involved in the Apollo digital torquing technique.

By way of recapitulation, let us enumerate the important considerations necessary to an accurate torquing system:

a) Current control

Circuitry and tolerances on components in the current control loop must guarantee super-accuracy in the current reaching the torquer.

b) Reluctance (and Inductance) control:

Mechanical tolerances on the torque generator must be very precise. Materials used in core construction must be carefully chosen to minimize hysteresis, non-linearity, and temperature sensitivity problems.

In addition, it is necessary to minimize the effects of the torquing system on the other gyro functions. Such characteristics as residual torques and elastic restraints are undesirable.

The Apollo torquing technique was designed with these considerations as a guide. As a result, gimbals of the Inertial Measurement Unit can be positioned to within 1000 ppm (0.1%) of the commanded angle, insuring accurate pre-launch and inflight alignment of the stable platform.

E-1942

DISTRIBUTION LIST

Internal:

M. Adams (MIT/GAEC)
J. Alexshun
J. Aronson (Lincoln)
R. Battin
R. Booth
P. Bowditch/F. Siraco
A. Boyce
G. Bukow
R. Byers
N. Cluett
E. Copps
R. Crisp
J. Dahlen
J. DeLisle
J. Feldman (5)
J. B. Feldman
P. Felleman
S. Felix
J. Flanders (MIT/KSC)
J. Fleming
G. Garcia
J. Gilmore
F. Grant
E. Hall
Eldon Hall
T. Hemker (MIT/NAA)
D. Hoag
F. Houston
L. B. Johnson
M. Johnston
A. Koso
M. Kramer
A. Laats
M. Lanman
L. Larson
S. Laquidara (MIT/FOD)
J. Lawrence (MIT/GAEC)
T. J. Lawton
T. M. Lawton (MIT/MSC)
D. Lickly
L. Martinage
G. Mayo
J. McNeil
R. McKern
James Miller
John Miller
J. Nevins
J. Nugent
E. Olsson
P. Palmer
R. Ragan
E. Schwarm
N. Sears
J. Shillingford
W. Shotwell (MIT/AC)
J. Sitomer
W. Stameris
J. Suomala
R. Therrien
M. Trageser
R. Weatherbee
L. Wilk
R. Woodbury
W. Wrigley
Apollo Library (2)
MIT/IL Library (6)

External:

W. Rhine (NASA/MSC) (2)

NASA/RASPO (1)

T. Heuermann (GAEC/MIT) (1)

AC Electronics (3)

Kollsman (2)

Raytheon (2)

Major H. Wheeler (AFSC/MIT) (1)

MSC:

National Aeronautics and Space Administration (25 + 1R)
Manned Spacecraft Center
Apollo Document Distribution Office (PA2)
Houston, Texas 77058

LRC:

National Aeronautics and Space Administration (2)
Langley Research Center
Hampton, Virginia
Attn: Mr. A.T. Mattson

GAEC:

Grumman Aircraft Engineering Corporation (3 + 1R)
Data Operations and Services, Plant 25
Bethpage, Long Island, New York
Attn: Mr. E. Stern

NAA:

North American Aviation, Inc. (18 + 1R)
Space and Information Systems Division
12214 Lakewood Boulevard
Downey, California
Attn: Apollo Data Requirements AE99
Dept. 4-096-704 (Bldg. 6)

NAA RASPO:

NASA Resident Apollo Spacecraft Program Office (1)
North American Aviation, Inc.
Space and Information Systems Division
Downey, California 90241

AC RASPO:

National Aeronautics and Space Administration (1)
Resident Apollo Spacecraft Program Officer
Dept. 32-31
AC Electronics Division of General Motors
Milwaukee 1, Wisconsin
Attn: Mr. W. Swingle

Defense Contract Administration (1)
Service Office, R
Raytheon Company
Hartwell Road
Bedford, Massachusetts 01730

Mr. S. Schwartz (1)
DOD, DCASD, Garden City
605 Stewart Avenue
Garden City, L.I., New York
Attn: Quality Assurance

Mr. D.F. Kohls (1)
AFPRO (CMRKKA)
AC Electronics Division of General Motors
Milwaukee 1, Wisconsin 53201